Measuring the Thermal Conductivity of a Single Carbon Nanotube

Motoo Fujii,[1] Xing Zhang,[1,*] Huaqing Xie,[1] Hiroki Ago,[1] Koji Takahashi,[2] Tatsuya Ikuta,[2] Hidekazu Abe,[3] and Tetsuo Shimizu[3]

[1]*Institute for Materials Chemistry and Engineering, Kyushu University, Kasuga 816-8580, Japan*
[2]*Graduate School of Engineering, Kyushu University, Fukuoka 812-8581, Japan*
[3]*Nanotechnology Research Institute, National Institute of Advanced Industrial Science and Technology, Tsukuba 305-8562, Japan*

(Received 13 April 2005; published 2 August 2005)

Although the thermal properties of millimeter-sized carbon nanotube mats and packed carbon nanofibers have been readily measured, measurements for a single nanotube are extremely difficult. Here, we report a novel method that can reliably measure the thermal conductivity of a single carbon nanotube using a suspended sample-attached T-type nanosensor. Our experimental results show that the thermal conductivity of a carbon nanotube at room temperature increases as its diameter decreases, and exceeds 2000 W/mK for a diameter of 9.8 nm. The temperature dependence of the thermal conductivity for a carbon nanotube with a diameter of 16.1 nm appears to have an asymptote near 320 K. The present method is, in principle, applicable to any kind of a single nanofiber, nanowire, and even single-walled carbon nanotube.

DOI: 10.1103/PhysRevLett.95.065502 PACS numbers: 81.07.De, 65.80.+n

As a typical one-dimensional (1D) nanostructure material, carbon nanotubes (CNTs) that have potential applications in electronic, optical, and energy conversion devices have received considerable attention since their discovery [1]. The electrical and mechanical properties have been investigated at a single nanotube level [2,3]. The thermal properties of CNTs are also of interest for basic science as well as for technological applications. Several groups [4–9] have measured the thermal properties of millimeter-sized CNT mats and packed carbon nanofibers. Although these studies can help us to understand the thermal properties of these materials, it is difficult to extract the intrinsic thermal properties of a single nanotube from these ''bulk'' measurements. Because of the difficulties in measurements of local temperature and heating rate for such a nanotube, conventional methods cannot be used for a single nanotube measurement. While an interesting measurement of the thermal transport through a multiwalled carbon nanotube (MWCNT) was done using a microdevice containing two suspended independent heaters [10], we had proposed a novel method using a sample-attached T-type sensor [11] that is able to measure the thermal conductivity of a single carbon fiber, metallic and nonmetallic wire, and even a single MWCNT or a bundle of several single-walled carbon nanotubes (SWCNTs). This method is considered to have the advantages of simplicity as well as high accuracy. It has been successfully used to measure the thermal conductivity of one single carbon fiber with a diameter of 10 μm or less [12]. However, because of the small size of carbon nanotubes, the sensor must be fabricated at nanoscale to obtain sufficient sensitivity. The connection between the nanosensor and nanotube also becomes one of the key points of the measurements.

In this Letter, we show how to use a sample-attached T-type nanosensor to measure the thermal conductivity of a single CNT in vacuum, how to manufacture a suspended nanofilm sensor with modern microelectromechanical system technology and how to connect a CNT to the nanofilm sensor with a special manipulation scanning electron microscope (SEM). We further report the measured thermal conductivity of nanofilm sensors and of three CNTs with different diameters.

Suspended platinum nanofilm sensors were fabricated on a multilayered film of electron beam resist/silicon oxide/silicon by electron beam lithography, electron beam physical vapor deposition, and isotropic/anisotropic etching processes, which are described elsewhere in detail [13]. The dimensions of the nanofilm sensors are varied in the ranges of 27.5–40.0 nm in thickness, 330–600 nm in width, and 5.3–5.7 μm in length, respectively. The gap between the nanofilm and substrate is 6 μm. The CNTs made by an arc-discharge evaporation method were chosen as the test samples. With the help of a manipulation SEM, the individual CNT that has a high quality and an available length was chosen and fixed to the nanotip of a metallic needle by using local focused electron beam irradiation. The structure and diameter of individual selected CNTs were further investigated by a high-resolution transmission electron microscopy before connecting a CNT and nanosensor. Using the same manipulation SEM and the local focused electron beam irradiation, one end of the CNT was attached to the center part of the nanosensor and the other to the heat sink. The local focused electron beam irradiation makes good thermal contact between the CNT and the nanofilm sensor and heat sink. Figure 1 shows a typical sample-attached T-type nanosensor including a hot Pt nanofilm sensor (NS), a CNT, and a heat sink (HS). The thickness, width, and length of the prepared nanofilm sensor [image in Fig. 1(b)] are 40.0 nm, 362 nm, and 5.67 μm, respectively. The diameter and length of the selected CNT are 9.8 nm and 3.70 μm, respectively. The hot nanofilm sensor serves simultaneously as a heater and a

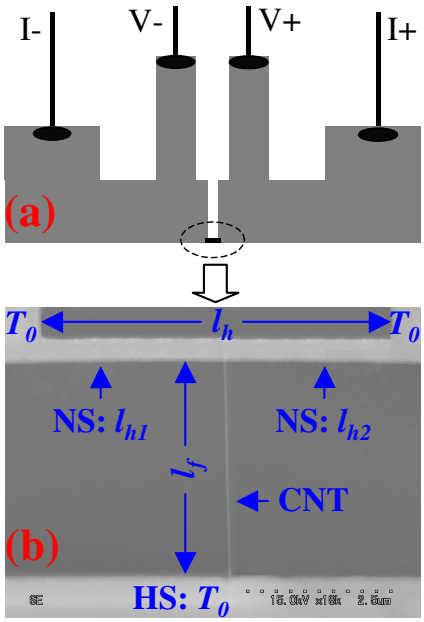

FIG. 1 (color online). Schematic diagram of the nanosensor and the scanning electron micrograph of a suspended CNT-attached T-type nanosensor.

thermometer to measure the average temperature of the nanofilm so that the local temperature of the junction point and the heat input to the CNT can be calculated based on the theoretical solution of one-dimensional heat conduction. The hot nanofilm sensor itself is heated by supplying a constant current. Since both ends of the hot nanofilm sensor and the end of the CNT at the heat sink side are supported with the Pt frames that have large heat capacities compared to those of the hot nanofilm and CNT, the temperatures at both ends of hot nanofilm sensor and the end of the CNT at the heat sink side can be maintained at the initial temperature, T_0, for the entire measurement. Because of the nanoscale effect of sensor and sample, our calculations have shown that the effects of the heat losses from the heat conduction of rarefied gas in vacuum and thermal radiation can be neglected. Based on the one-dimensional steady-state heat conduction model including the thermal contact resistance at the junction of the nanofilm and CNT, the volumetric average temperature rise of the nanosensor, ΔT_v, and the thermal conductivity of CNT, λ_f, can be expressed by

$$\Delta T_v = \frac{(l_{h1}^3 + l_{h2}^3) q_v}{12 l_h \lambda_h} + \frac{l_{h1} l_{h2} l_h A_h q_v (l_f + \lambda_f R_c)}{4\{l_{h1} l_{h2} \lambda_f A_f + l_h \lambda_h A_h (l_f + \lambda_f R_c)\}} \quad (1)$$

and

$$\lambda_f = \frac{l_f l_h \lambda_h A_h (l_h^3 q_v - 12 l_h \lambda_h \Delta T_v)}{l_{h1} l_{h2} A_f \{12 l_h \lambda_h \Delta T_v - q_v (l_{h1}^3 + l_{h2}^3)\} - l_h \lambda_h A_h R_c (l_h^3 q_v - 12 l_h \lambda_h \Delta T_v)}, \quad (2)$$

where A_f is the cross sectional area of the CNT, A_h is the cross sectional area of the nanofilm, l_f is the length of CNT between the two connecting points at the nanofilm and the heat sink, l_h is the length of the nanofilm, l_{h1} and l_{h2} are the lengths of the left- and right-hand sides of the nanofilm from the junction point, R_c is the thermal contact resistance, and λ_h is the thermal conductivity of the nanofilm. q_v is the volumetric heat generation rate given by $q_v = IV/(wtl_h)$ and ΔT_v is obtained from $\Delta T_v = \Delta R/(\beta R_0)$, where w and t are the width and thickness, respectively, of the nanofilm, I and V are the heating current and voltage, R_0 is the electrical resistance of the nanofilm at 0 °C, ΔR is the electrical resistance increase of the nanofilm found by measuring the heating current and voltage, and β is the resistance-temperature coefficient of the nanofilm obtained from calibration. It is clear from Eq. (2) that we can obtain the thermal conductivity of the nanotube by measuring the volumetric average temperature rise and heat generation rate of the nanofilm for a nanofilm and nanotube with given dimensions and thermal contact resistance. In principle, the junction thermal contact resistance can also be measured by changing the length of the nanotube with a special manipulation SEM although this has been reported to be relatively small compared to the thermal resistance of a test sample [10]. Defining the ratio of the junction thermal contact resistance to the thermal resistance of CNT $C_f = R_c/(l_f/\lambda_f)$, the thermal conductivity of CNT is given by

$$\lambda_f = \frac{l_f l_h \lambda_h A_h (l_h^3 q_v - 12 l_h \lambda_h \Delta T_v) + C_f l_f l_h \lambda_h A_h (l_h^3 q_v - 12 l_h \lambda_h \Delta T_v)}{l_{h1} l_{h2} A_f \{12 l_h \lambda_h \Delta T_v - q_v (l_{h1}^3 + l_{h2}^3)\}}. \quad (3)$$

If $R_c = 0$, that is $C_f = 0$, Eq. (3) is reduced to

$$\lambda_{f0} = \frac{l_f l_h \lambda_h A_h (l_h^3 q_v - 12 l_h \lambda_h \Delta T_v)}{l_{h1} l_{h2} A_f \{12 l_h \lambda_h \Delta T_v - q_v (l_{h1}^3 + l_{h2}^3)\}}. \quad (4)$$

Equation (4) gives the lowest bound of the intrinsic thermal conductivity, λ_{f0}, of the CNT. The influence of the junction thermal contact resistance on the determination of the thermal conductivity of the CNT is calculated by $\varepsilon = (\lambda_f - \lambda_{f0})/\lambda_{f0} = C_f$. Therefore, the intrinsic thermal conductivity becomes close to the lowest bound if the junction thermal contact resistance is relatively small compared to the thermal resistance of the CNT.

It is known that the electrical and thermal properties of nanoscale materials are very different from the bulk values due to the structure defect and boundary scattering [14–17]. It is essential to determine the electrical and thermal properties of Pt nanofilm used in our experiments. Before the CNT was attached to the nanosensor, the resistance-temperature coefficient and thermal conductivity of the

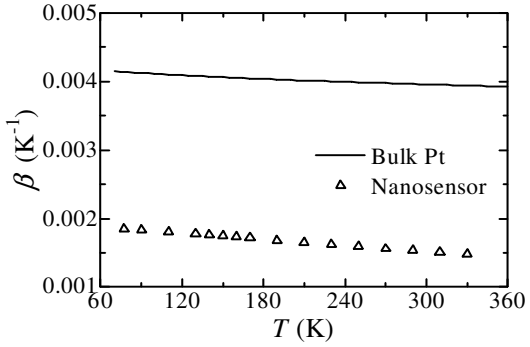

FIG. 2. Resistance-temperature coefficient of nanosensor (t = 27.5 nm, w = 332 nm, l_h = 5.37 μm).

nanofilm were measured in advance by $\beta = \Delta R/(R_0 \Delta T)$ and $\lambda_{ns} = {l_h}^2 q_v/(12\Delta T_v)$, and shown in Figs. 2 and 3, respectively. The electrical resistance of the nanosensor was measured by a four-wire technique as shown in Fig. 1(a). The maximum uncertainty of the measured electrical resistance values is within 0.005%. The uncertainty of the thermal conductivity can arise from errors in measurements of voltage, current, temperature, and dimensions of the nanofilm. The width and length of the nanofilm are measured with a scanning electron microscope, and the film thickness is measured with a calibrated quartz crystal thin-film thickness monitor (CRTM-7000 with the resolution of 0.01 nm). The error caused by the dimension measurements is estimated to be less than $\pm 3\%$. The overall error of the thermal conductivity is estimated to be within $\pm 5\%$. It is seen from Figs. 2 and 3 that the measured resistance-temperature coefficients and thermal conductivities of the nanofilm sensor are significantly lower than the corresponding bulk values. The measured resistance-temperature coefficient of 0.0015 K^{-1} at 290 K is less than half of that of the corresponding bulk value of 0.0039 K^{-1}. The measured thermal conductivity of 29.5 W/mK at 290 K is also less than half of the corresponding bulk value of 71.4 W/mK. Previous studies state that since the thermal conductivity of pure bulk sample is proportional to the electrical conductivity of the same samples via the Wiedemann-Franz law, the reduced thermal conductivity of thin films must also have the same proportionality with the reduced electrical conductivity of the same films [18–22]. It is worth noting, however, that the ratio of the thermal conductivity to the electrical conductivity, calculated from the present measurements, is about 1.66×10^{-5} W Ω/K at 300 K, whereas that of the bulk platinum is about 7.5×10^{-6} W Ω/K. This remarkable discrepancy indicates that the relation between the thermal conductivity and electrical conductivity of these nanoscale metallic thin films does not follow the Wiedemann-Franz law for the bulk metals. The effects of material type, fabrication method, and film sizes need to be taken into account. Therefore considerable care must be taken when we estimate the thermal conductivity from the electrical conductivity of metallic nanofilms.

The volumetric average temperature rise of the nanosensor as a function of heating rate ($Q = IV$) is shown in Fig. 4. The closed circles represent the results with a CNT attached to the nanosensor, the open ones without a CNT. It is clearly seen that the average temperature rise with a CNT is lower than that without a CNT. The slope used for the calculation of the thermal conductivity is determined by a linear least-squares fit of experimental data and the thermal conductivity is calculated from Eq. (4). The thermal conductivities of three different diameters of CNTs at room temperature are shown in Fig. 5. The cross sectional area of the CNT in Eq. (4) is calculated by (a) $A_f = \pi {d_o}^2/4$ (the same definition as others) and (b) $A_f = \pi({d_o}^2 - {d_i}^2)/4$, respectively, where d_o is the outer diameter of the CNT and d_i is the diameter of the inner lumen. The effect of the inner lumen on the thermal conductivity estimation increases as the outer diameter of the CNT decreases. The thermal conductivity is up to 1.37 times for the outer diameter of 9.8 nm if the area of the inner lumen is subtracted. It is noted that the present results are the lowest bounds of the intrinsic thermal conductivity without considering the effect of the junction thermal contact resistance. Although it is extremely difficult to measure the junction thermal contact resistance, simultaneous measurements of the junction thermal contact resistance and thermal conductivity of CNT are being attempted through changing the length of the CNT with the manipulation SEM. It is clearly seen

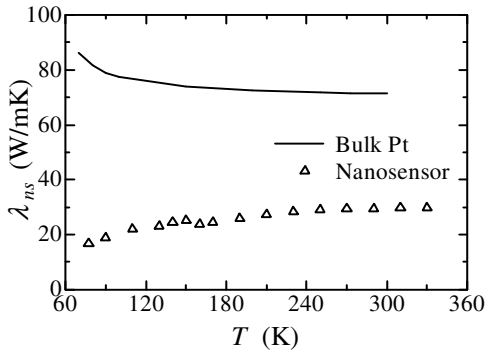

FIG. 3. Thermal conductivity of nanosensor (t = 27.5 nm, w = 332 nm, l_h = 5.37 μm).

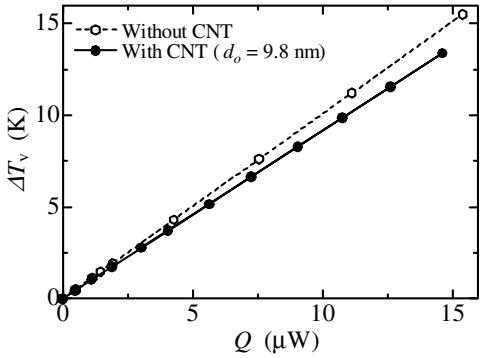

FIG. 4. Temperature rise versus heating rate measured in a vacuum.

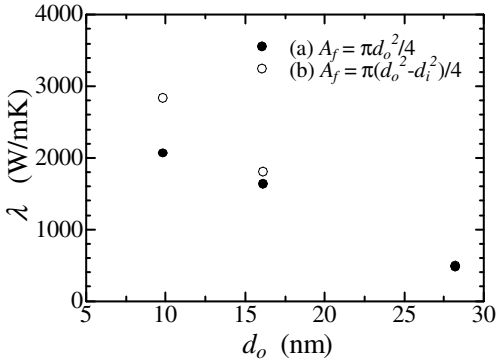

FIG. 5. Thermal conductivity of a single carbon nanotube at different diameters [(a) $d_o = 9.8$ nm, $d_i = 5.1$ nm, $l_f = 3.70$ μm; (b) $d_o = 16.1$ nm, $d_i = 4.9$ nm, $l_f = 1.89$ μm; (c) $d_o = 28.2$ nm, $d_i = 4.2$ nm, $l_f = 3.60$ μm].

from Fig. 5 that the thermal conductivity of a CNT at room temperature increases as its diameter decreases. The present result for a CNT with a diameter of 9.8 nm is 2069 W/mK, whereas the previous bulk measurement on a MWCNT mat using a self-heating method [4] gives an estimate of only 20 W/mK. The diameter-dependent thermal conductivity indicates that the interactions of phonons and electrons between multiwalled layers affect the thermal conductivity. The thermal conductivity increases as the number of multiwalled layers decreases. A single-walled carbon nanotube is expected to have much higher thermal conductivity.

Figure 6 represents the temperature dependence of the thermal conductivity for a CNT with a diameter of 16.1 nm. The open and closed circles represent the different results obtained by two definitions of the cross sectional areas of the CNT as mentioned above. The measured thermal conductivity increases with an increase in temperature and appears to have an asymptote near 320 K. This tendency is the same as those obtained previously [10], which is attributed to the onset of umklapp phonon scattering.

In conclusion, we have successfully measured the thermal conductivity of a single MWCNT with a suspended sample-attached T-type nanosensor. The present method is, in principle, applicable to any kind of a single nanofiber,

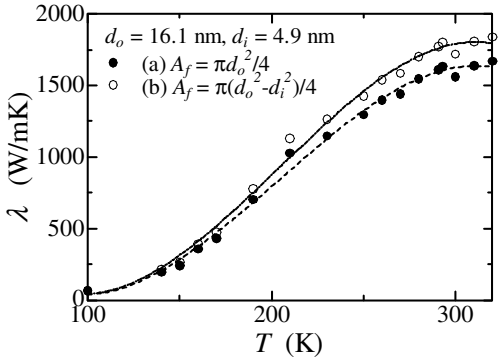

FIG. 6. Thermal conductivity of a single carbon nanotube at 100–320 K.

nanowire, and even SWCNT. Because of the difficulty in manipulation technique for an individual SWCNT, experiments intended to measure a bundle of several SWCNTs are being attempted. Simultaneous measurements of the junction thermal contact resistance and thermal conductivity of a CNT are also being attempted by changing the length of the sample with a special manipulation SEM.

This work is supported partly by the Grant-in-Aid for Scientific Research B15360114 from the Ministry of Education, Science, Sports and Culture of Japan.

*Corresponding author.
Electronic address: xzhang@cm.kyushu-u.ac.jp

[1] S. Iijima, Nature (London) **354**, 56 (1991).
[2] C. H. Olk and J. P. Heremans, J. Mater. Res. **9**, 259 (1994).
[3] C. Dekker, Phys. Today **52**, No. 5, 22 (1999).
[4] W. Yi, L. Lu, Z. Dian-lin, Z. W. Pan, and S. S. Xie, Phys. Rev. B **59**, R9015 (1999).
[5] J. Hone, M. Whitney, C. Piskoti, and A. Zettl, Phys. Rev. B **59**, R2514 (1999).
[6] J. Hone, M. C. Llaguno, N. M. Nemes, A. T. Johnson, J. E. Fischer, D. A. Walters, M. J. Casavant, J. Schmidt, and R. E. Smalley, Appl. Phys. Lett. **77**, 666 (2000).
[7] J. Hone, M. C. Llaguno, M. J. Biercuk, A. T. Johnson, B. Batlogg, Z. Benes, and J. E. Fischer, Appl. Phys. A: Mater. Sci. Process. **74**, 339 (2002).
[8] D. J. Yang, Q. Zhang, G. Chen, S. F. Yoon, J. Ahn, S. G. Wang, Q. Zhou, Q. Wang, and J. Q. Li, Phys. Rev. B **66**, 165440 (2002).
[9] H. Q. Xie, H. Gu, M. Fujii, and X. Zhang, Int. J. Thermophys. (to be published).
[10] P. Kim, L. Shi, A. Majumdar, and P. L. McEuen, Phys. Rev. Lett. **87**, 215502 (2001).
[11] X. Zhang, S. Fujiwara, and M. Fujii, High Temp. High Press. **32**, 493 (2000).
[12] X. Zhang, S. Fujiwara, and M. Fujii, Int. J. Thermophys. **21**, 965 (2000).
[13] X. Zhang, H. Q. Xie, M. Fujii, K. Takahashi, H. Ago, T. Shimizu, and H. Abe, Jpn. J. Thermophys. Prop. **19**, 9 (2005).
[14] T. Yamane, Y. Mori, S. Katayama, and M. Todoki, J. Appl. Phys. **82**, 1153 (1997).
[15] S. R. Mirmira and L. S. Fletcher, J. Thermophys. Heat Transfer **12**, 121 (1998).
[16] D. G. Cahill, W. K. Ford, K. E. Goodson, G. D. Mahan, A. Majumdar, H. J. Maris, R. Merlin, and S. R. Phillpot, J. Appl. Phys. **93**, 793 (2003).
[17] X. Zhang, H. Q. Xie, M. Fujii, H. Ago, K. Takahashi, T. Ikuta, H. Abe, and T. Shimizu, Appl. Phys. Lett. **86**, 171912 (2005).
[18] C. Kittel, *Introduction to Solid State Physics* (Wiley, New York, 1986), 6th ed.
[19] C. L. Tien, B. F. Armaly, and P. S. Jagannathan, *Thermal Conductivity* (Plenum Press, New York, 1969).
[20] C. R. Tellier and A. J. Tosser, *Size Effects of Thin Films* (Elsevier Publishing, New York, 1982).
[21] P. Nath and K. L. Chopra, Thin Solid Films **20**, 53 (1974).
[22] B. M. Clemens, G. L. Eesley, and C. A. Paddock, Phys. Rev. B **37**, 1085 (1988).